Oxidant Production over Antarctic Land and its Export (OPALE) project: An overview of the 2010-2011 summer campaign

Susanne Preunkert, Gérard Ancellet, Michel R. Legrand, Alexandre Kukui, Michael Kerbrat, Roland Sarda-Estève, Valérie Gros, Bruno Jourdain

Oxidant Production over Antarctic Land and its Export (OPALE) project: An overview of the 2010–2011 summer campaign

Susanne Preunkert,[1] Gérard Ancellet,[2] Michel Legrand,[1] Alexandre Kukui,[2] Michael Kerbrat,[1] Roland Sarda-Estève,[3] Valérie Gros,[3] and Bruno Jourdain[1]

[1]   This paper summarizes the objectives and setting of the OPALE (Oxidant Production over Antarctic Land and its Export) project during summer 2010/2011 at Dumont d'Urville. The primary goal of the campaign is to characterize the oxidizing environment of the atmospheric boundary layer along the coast of East Antarctica. A summary of the relevant field chemical measurements is presented including the carbon monoxide and ammonia records that are used here to identify local influences due to station activities and penguin emissions. An overview of the basic meteorological conditions experienced by the site is presented including the results from the trajectory/dispersion model FLEXPART to highlight which types of air mass were sampled (marine boundary layer versus continental Antarctic air). The results of the FLEXPART analysis demonstrate that high ozone levels and related changes in the OH concentrations are associated with the transport of continental air to DDU. Finally, three companion papers are introduced. A first paper is dedicated to the impact of local penguin emissions on the atmospheric budget of several oxygenated volatile organic compounds. The second paper reports on HONO levels that were measured for the first time in Antarctica by using the long path absorption photometer (LOPAP) technique. Finally, in a third paper, major findings on the HO_x levels are detailed, leading to the overall conclusion that the photochemistry at coastal East Antarctica is strongly driven by an efficient HO_x chemistry compared to the situation at other coastal Antarctic regions.

Citation: Preunkert, S., G. Ancellet, M. Legrand, A. Kukui, M. Kerbrat, R. Sarda-Estève, V. Gros, and B. Jourdain (2012), Oxidant Production over Antarctic Land and its Export (OPALE) project: An overview of the 2010–2011 summer campaign, *J. Geophys. Res.*, *117*, D15307, doi:10.1029/2011JD017145.

1.   Introduction

[2] In addition to stable water isotopes recorded in Antarctic ice cores, valuable paleo-climate information can be derived from studies of various gases encapsulated in ice bubbles and chemical compounds preserved in the ice lattice. In this context, a review of the ionic ice composition related to deposition of aerosol and water-soluble trace gases can be found in *Legrand and Mayewski* [1997]. Clearly, the signals of aerosol or reactive trace gas species recorded in the ice depend not only on the source strength and snow accumulation but also on numerous processes that act during transport

toward the site and, for some species, on post depositional processes. Sulfur, one of the critical species for which an overall understanding of its biogeochemical cycle is needed for climate change studies [*Charlson et al.*, 1987] is also a key component of aerosol archived in polar ice. Motivated by a possible atmosphere/ocean sulfur link, numerous ice cores studies focused on past change of methanesulfonate (MSA) and sulfate, two aerosol species produced by the oxidation of DMS emitted by marine biota [*Legrand*, 1997]. The atmospheric behavior of DMS under Antarctic conditions being poorly known, most of these studies had however assumed a straightforward relation between oceanic DMS emissions and the ice content of sulfate and MSA.

[3] With the aim to investigate the role of climate on the sulfur cycle, long-term atmospheric observations of aerosol had been initiated at coastal Antarctic stations since 1983 at Neumayer [*Wagenbach*, 1996] and 1991 at Dumont d'Urville [*Jourdain and Legrand*, 2002; *Preunkert et al.*, 2007] (Figure 1). The lack of knowledge of the atmospheric behavior of DMS also stimulated studies of the DMS cycle including DMSO, SO_2, sulfate and MSA measurements. This was done at coastal Antarctic sites like Dumont d'Urville [*Jourdain and Legrand*, 2001] and during the SCATE

---

[1]CNRS/UJF – Grenoble 1, Laboratoire de Glaciologie et Géophysique de l'Environnement, UMR 5183, Grenoble, France.

[2]Laboratoire des Atmosphères, Milieux, Observations Spatiales, Guyancourt, France.

[3]Laboratoire des Sciences du Climat et de l'Environnement, Gif sur Yvette, France.

Corresponding author: S. Preunkert, CNRS/UJF – Grenoble 1, Laboratoire de Glaciologie et Géophysique de l'Environnement, UMR 5183, Grenoble FR-38041, France. (preunkert@lgge.obs.ujf-grenoble.fr)
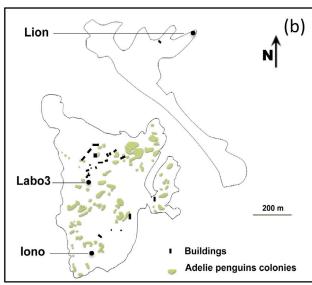
Figure 1. (a) Map of Antarctica showing the Dumont d'Urville and Concordia sites and other stations mentioned in this paper. (b) Map of local area around Dumont d'Urville indicating the location of the three sampling sites, "labo 3" and "iono" set up on the "Ile des Pétrels" and "lion" on the small island located further northeast. Locations of buildings and penguin colonies present on the "Ile des Pétrels" are reported in black and gray, respectively.

(Sulfur Chemistry in the Antarctic Troposphere Experiment) project conducted at Palmer [*Berresheim and Eisele*, 1998]. At this site, and for the first time in Antarctica, OH radicals were measured indicating a mean 24 h concentration of $1.1 \ 10^5$ radicals cm^{-3} [*Jefferson et al.*, 1998] in February. At Halley, OH measurements indicated similar values with a mean OH concentration of $4 \ 10^5$ radicals cm^{-3} in January [*Bloss et al.*, 2007]. These values are consistent with a low OH production driven by the ozone photolysis and, as expected in these low NO_x environments, an absence of HO_x

recycling and O_3 production. To date, at Dumont d'Urville O_3 levels sometimes reach values as high as 35 ppbv in summer, largely exceeding the background value of 15 ppbv observed at other coastal sites [*Legrand et al.*, 2009]. This suggests that, in contrast to the situation at other coastal sites, air masses advected to this East Antarctic coastal site in summer had experienced a photochemical ozone production.

[4] On the Antarctic plateau year-round aerosol studies are more scattered than at the coast [*Tuncel et al.*, 1989; *Weller and Wagenbach*, 2007; *Preunkert et al.*, 2008]. The SCATE campaign at Palmer suggested that, given the OH level at the coast, significant amount of DMS may reach the Antarctic plateau, therefore a follow up project, ISCAT (Investigation of Sulfur Chemistry in Antarctica Troposphere) dedicated to the sulfur chemistry was conducted at the South Pole. However, unexpected very low (below less than 2 pptv) DMS values were found during the first campaign (ISCAT 1998) [*Davis et al.*, 2004]. These low DMS values tended to suggest a faster oxidation during the transport from oceanic source regions to the site than initially assumed. The existence of an oxidizing canopy over the South Pole region was indeed pointed out by measurements carried out during this first ISCAT campaign. Up to $4 \ 10^6$ OH radicals cm^{-3} were measured [*Mauldin et al.*, 2001a], making the South Pole boundary layer as oxidative as the remote tropical marine boundary layer [*Mauldin et al.*, 2001b], which is well beyond any model prediction considering the very dry Antarctic environment. *Chen et al.* [2001] and *Davis et al.* [2001] showed that the high levels of NO generated by the photolysis of nitrate present in surface snow layers, profoundly perturb the chemistry of the South Pole atmosphere that was considered to be the most pristine planetary boundary layer on Earth. The NO emission from the snowpack is thought to mainly account for these unexpectedly high values of OH but additional observations made during ISCAT 2000 demonstrated that not only NO emissions contribute to the observed high level of OH but also re-emissions of HCHO and H_2O_2 [*Chen et al.*, 2004]. Also, the importance of HONO as a source of OH remains unclear. The relevance of these processes identified at the South Pole at the continental scale requires further studies, particularly over the East Antarctic plateau. Indeed some data from aircraft observations during ANTCI 2003 suggest that over the East Antarctic plateau even higher NO emissions persist [*Davis et al.*, 2008].

[5] The need to characterize the oxidative capacity of the atmosphere in the vast region of East Antarctica motivated the OPALE initiative with investigations both at the top of the high plateau (Concordia) and at the East coast (Dumont d'Urville). The top of the East Antarctic plateau is a region where processes are suspected to differ from those identified at the South Pole. For instance, in contrast to the South Pole experiencing 24-h sunlight, the solar irradiance at Concordia has a strong diurnal cycle. Concordia is also the inland site where the longest sulfur derived aerosol records has been extracted from deep ice cores [*Wolff et al.*, 2006]. Regarding coastal site observations, it is suspected that the oxidative capacity of the atmosphere is different in Eastern Antarctica due to the frequent occurrence of katabatic flow. This has to be considered in studies dealing with year-round observations carried out at coastal Antarctic sites [see, e.g., *Weller et al.*, 2011]. Experimental studies at the East Antarctic

Table 1. OPALE Atmospheric Measurements Made During the 2010/11 Summer Season[a]

Compound	Investigator[b]	Technique[c]	Quantification Limit	Sampling Time Period	Sampling Location
OH	LATMOS	CIMS	0.03 pptv (2 min)	Dec 25 – Jan 14	iono
HO_2+RO_2			0.06 pptv		
HONO	LGGE	LOPAP	1.5 pptv (9 min)	Dec 22 – Jan 18	Concordia
				Feb 9 – Feb 23	iono
HCHO	LGGE	Aerolaser AL 4021	50 pptv (30 s)	Dec 23 – Feb 09	iono lion
H_2O_2	LGGE	Aerolaser AL2021	50 pptv (30 s)	Dec 26 – Feb 08	labo 3
CH_3OOH			50 pptv (30 s)		
NH_3	LGGE	AIM	45 pptv (1 h)	Dec 25 – Dec 30	labo 3
HCOOH		URG 9000D	1 pptv (1 h)	Jan 02 – Feb 06	iono
CH_3COOH			1 pptv (1 h)		
Aerosols			2 pptv (1 h)		
CH_3CHO	LSCE	PTR-MS	25 pptv (60 s)	Dec 31 – Jan 24	iono
CH_3COCH_3		Ionicon	11 pptv (60 s)		
Black Carbon	LSCE	Magee Scientifique Portable Aethalometer AE42	60 pptv (5 min)	Dec 23 – Jan 24	iono
CO	LSCE	RGA3 Trace Analytical	6 ppbv (3 min)	Jan 04 – Jan 24	iono
DMS	LGGE	Gas chromatograph HP6890	13 pptv (canister)	Dec 25 – Feb 24	labo 3
O_3	LGGE	Thermo Electron 49I	1 ppbv (15 min)	Dec 25 – Feb 24	labo 3

[a]Quantification limits are estimated for 3σ.

[b]LATMOS is Laboratoire des Atmosphères, Milieux, Observations Spatiales, LGGE is Laboratoire de Glaciologie et Géophysique de l'Environnement, and LSCE is Laboratoire des Sciences du Climat et de l'Environnement.

[c]CIMS refers to chemical ionisation mass spectrometry, LOPAP to long path absorption photometer, AIM to ambient ion monitor, and PTR-MS to proton transfer mass spectrometry.

coast are then needed to understand to what extend the very oxidizing inland air masses can reach coastal regions where large oceanic DMS emissions take place.

2. OPALE 2010–2011 Site Location and Instrumental Techniques

[6] The OPALE field campaign was initially planned to take place during November and December 2010 at Concordia (central Antarctica, 75°06′S, 123°33′E, 3223 m above sea level) located 1100 km away from the nearest coast of East Antarctica and in January 2011 at the coastal site of Dumont d'Urville (66°40′S, 140°01′E, 40 m above the sea level). Measurements of OH, the sum of HO_2+RO_2, NO, NO_2, HONO, O_3, H_2O_2, HCHO, O and N isotopes on nitrates were planned. Due to logistical problems, which followed a helicopter accident (occurred 28th October 2010), there was a major reconfiguring of the OPALE 2010–2011 field campaign. Since there was very limited possibility to transport researchers and their scientific cargo to the Concordia site, the 2010–2011 field season was focused on the evaluation of the oxidative properties of the atmosphere at the coastal East Antarctic site of Dumont d'Urville (DDU). Furthermore, limitation of the scientific cargo and number of scientists obliged us to cancel NO_x measurement at the coast. On the other hand, despite all problems, the HONO study started at Concordia end of 2010 and took place at DDU during the second half of February 2011. The overall characterization of the atmosphere at Concordia with respect to oxidants was postponed to the 2011/2012 summer campaign.

2.1. Measurement Locations at DDU

[7] Table 1 provides a summary of the OPALE 2010/2011 measurements, including the principle investigators, the quantification limit of the instruments, and where and over what time period it was deployed. The main sampling period at DDU took place from the end December to mid January.

Some measurements continued until the end of January or the beginning of February. Back from Concordia the HONO device was run at DDU during the second half of February. Most of relevant chemical measurements were made at the site denoted "iono" in Figure 1. This place was preferred rather than the one at the chemical laboratory (denoted "labo 3") to minimize the frequency of air masses contaminated by station activities that reach the sampling lines. Indeed during the SCATE campaign, *Jefferson et al.* [1998] reported large OH spikes (up to $4 \cdot 10^6$ radicals cm^{-3} instead of $\sim 7 \cdot 10^5$ radicals cm^{-3} under clean air conditions at noon) when local pollution (NO emissions) reached the sampling building. As discussed by *Kerbrat et al.* [2012], HONO concentrations were also found to be sensitive to station activities. As previously discussed by *Legrand et al.* [2009], ozone measurements made at "labo 3" since 2004 are not very sensitive to station activities and are only in very rare occasions impacted by the plume of the station power supply, either when wind was blowing from 35°E (Figure 1) or at low wind speeds. No evidence that H_2O_2 and CH_3OOH are sensitive to station activities was observed, thus their measurements were also done at "labo 3."

[8] In addition to these man-made activities a second local source of atmospheric contamination exists at DDU. Indeed, as already shown by *Legrand et al.* [1998], high concentrations of ammonia are observed at DDU from end of October to late February in relation with the presence of large Adélie penguin colonies. On the basis of carboxylic acids and ammonia data collected since 1999 at "labo 3," *Legrand et al.* [2012] demonstrated that in addition to ammonia several oxygenated volatiles organic compounds (OVOCs) including light carboxylic acids are also emitted by ornithogenic soils (guano-enriched soils). The authors showed that these local emissions are highly dependent on weather conditions. The bacterial decomposition of guano into ammonia and volatile organic compounds is indeed strengthened by the occurrence of snowfalls followed or accompanied by mild
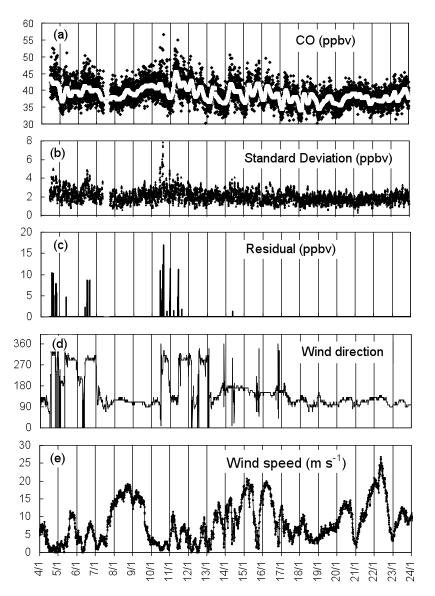
Figure 2. Carbon monoxide data and wind conditions at DDU in January 2011. (a) CO mixing ratios at "iono," dots refer to 3 min averages and the thick white line to the smoothed profile (robust spline). (b) Standard deviations of 10 successive 3 min data of the detrended data set. (c) CO concentrations which can be attributed to station contamination (see text). (d) Wind direction expressed in degree (see Figure 1). (e) Wind speed. Wind conditions are 10 min averages.

temperatures, providing there enough moisture in ornithogenic soils.

[9] In the two following sections the actual impact of these two sources during the sampling period is evaluated by using chemical records.

2.2. Station Activities

[10] With the aim to evaluate the degree of contamination of "iono" by station activities an aethalometer was deployed there. In addition to large spikes of a few hundreds of ng cm^{-3} obviously related to helicopter aviation nearby the sampling site, persistent very high values (several thousands ng m^{-3}) were recorded for example January 7th at night and January 8th morning. This event (not shown) took place during a severe storm when large amounts of brown material from ornithogenic soils were eroded, as it was also clearly

visible on the fresh snow surface. Consequently, the aethalometer was not a suitable method to monitor station contamination at DDU.

[11] With the aim to evaluate the sinks of OH [see *Kukui et al.*, 2012] carbon monoxide was monitored at "iono." Its record (Figure 2) indicates mixing ratios generally ranging between 33 and 50 ppbv. The lowest values close to 35 ppbv seen January 5th, 17th, 18th, and 19th (Figure 2) correspond to air mass advected from inland Antarctica as discussed in section 3.2.2. These low CO values are consistently close to those observed at the end of December at the inland Antarctic site of the South Pole (34.5 ppbv [*Davis et al.*, 2004]). The impact of station activities at "iono" was tentatively examined by scrutinizing the 3 min averages CO mixing ratios record as a function of local wind conditions. As seen in Figure 2a the CO values tend to be more scattered during the

first half of the period when wind was either very weak or blowing from the station (wind direction ranging between 0 and 45° East, see Figure 1) than after January 17th when wind was continuously blowing from the continent (wind direction of 90–180° East, Figure 1). The standard deviation of CO measurements evaluated by repeating analysis of air from high-pressure cylinders for the range of mixing ratios observed at DDU was found to be close to 2.0 ppbv. This value was compared to the scattering of CO values measured during the campaign, the latter being de-trended from variations related to changes in the atmospheric air composition. To achieve this de-trending of the data set, a robust spline smoothing [*Bloomfield and Steiger*, 1983] (Figure 2a) was applied and afterwards subtracted from the raw data set (3 min averages). Finally a running standard deviation was calculated (with a window size of 10) along the de-trended record (Figure 2b). Over the last seven days of the CO sampling period, wind conditions prevented the site from contamination by station activities and on average the standard deviation of residual values remained close to 1.8 ppbv, consistently with the accuracy of CO measurements. As seen in Figure 2b the standard deviation of the detrended CO data ranged from 0.3 to 3.7 ppbv over days during which no contamination by station activities is expected (from January 7th to January 9th and after January 17th). However, the standard deviation was sometimes also higher than 4 ppbv, particularly January 4th in the afternoon and January 6th in the morning as well as January 10th in the afternoon. All these events took place under low wind speed conditions, suggesting that sporadic arrivals of contaminated plumes at the sampling site at that time were responsible for enhanced scattering of the CO mixing ratios. In Figure 2c we reported the increase of CO mixing ratios that can be attributed to these arrivals of polluted air masses, determined as the CO concentrations of the de-trended data set during periods in which the standard deviation was higher than 4 ppbv. It appears that station activities can enhance CO levels by some 10 ppbv but these events generally remained limited to less than one hour.

2.3. Local Penguin Emissions

[12] Located at the southern headland of "Ile des Pétrels," the "iono" site is less exposed to penguin emissions than the "labo 3" site where penguins are present all around (Figure 1). As discussed in details in *Legrand et al.* [2012] the impact of the penguin emissions on measurements made at "iono" is highly variable depending on wind direction. For instance the drop of ammonia levels January 5th in the afternoon correspond to a jump of wind direction from the 0–60°E, a sector occupied by the largest penguin colonies of the Archipelago, to 270°E, an oceanic sector free of penguins for instance (Figure 3). In spite of this strong influence of wind conditions, the ammonia record at "iono" clearly shows a recovery of high ammonia concentrations up to 10,000–30,000 ng m^{-3} following the strong snowstorm that occurred January 8th to January 10th in the morning. These humid weather conditions have likely strengthened bacterial decomposition of uric acid as suggested by the strong increase of ammonia concentrations.

[13] As shown in *Legrand et al.* [2012], acetic acid concentrations at "iono" reached 5000 ng m^{-3} (around 2000 pptv, Table 2) when wind brought penguin emissions to the site. Other OVOCs found to be strongly impacted by penguin

emissions include acetone and acetaldehyde. For instance, between January 11th and January 14th when, as suggested by high levels of ammonia (Figure 3), the "iono" site was significantly impacted by penguin emissions, mixing ratios reached 270 ± 70 pptv of acetaldehyde and 230 ± 70 pptv of acetone (not shown), instead of 80 pptv and 130 pptv for background acetaldehyde and acetone levels, respectively. Among other OVOCs that may be of importance for the HOx budget is HCHO since its photolysis acts as a primary source of peroxy radicals [*Kukui et al.*, 2012]. However, *Legrand et al.* [2012] found that the contribution of local penguin emissions on the level of this species is far less dramatic than in the case of acetaldehyde, on averaged 10 pptv for a mean value of 170 pptv (Table 2). Finally, consistently with very low nitrite content observed in ornithogenic soils and a very high solubility of this species in alkaline soils [*Legrand et al.*, 2012] it was found that ornithogenic soils does not significantly disturb atmospheric HONO levels [*Kerbrat et al.*, 2012].

2.4. Instrumental Techniques

[14] The OH radical and the sum of hydroperoxy and organic peroxy radicals (HO_2+RO_2) were measured using the chemical ionization mass-spectrometer [*Kukui et al.*, 2008]. The detailed description of the instrument and details of its employment during this campaign are presented elsewhere [*Kukui et al.*, 2012]. These observations were complemented by measurements of direct HOx precursor species like HCHO, H_2O_2, and HONO.

[15] Formaldehyde measurements were made using an Aerolaser analyzer (Model AL 4021) that has a quantification limit of less than 50 pptv. The technique has been described in detail elsewhere [*Riedel et al.*, 1999; *Salmon et al.*, 2008]. In brief, gaseous HCHO is scrubbed into a diluted sulfuric acid solution followed by reaction with the Hantzsch reagent, a dilute mixture of acetyl acetone, acetic acid, and ammonium acetate. Aqueous-phase formaldehyde reacts with the Hantzsch reagent to produce a fluorescent compound that is detected at 510 nm.

[16] A fluorimetric two-channel technique, described in detail by *Lazrus et al.* [1985], was applied for determinations of hydroperoxides (Aerolaser, Model AL2021). Hereby the air first stripped in a buffer solution (pH of 5.8–6.0). In the first channel, the fluorimetric reagent (para-hydroxyphenylacetic acid) and horseradish peroxidase are added to determine the total amount of hydroperoxides. The produced fluorescent compound is detected at 415 nm. A distinction between hydrogen peroxide and organic hydroperoxides is achieved by selective destruction of H_2O_2 with the enzyme catalase in the second channel. As discussed by *Riedel et al.* [2000], no other organic peroxide than methylhydroperoxide (MHP, CH_3OOH) are present in remote marine areas and it can be assumed that the signal from the catalase channel corresponds to MHP.

[17] For the first time in Antarctica, HONO was measured using the long path absorption photometer (LOPAP) technique. In brief, after being stripped in an acid solution of sulphanilamide, HONO is derivatized using n-(1-naphthyl)-ethylenediamine-dihydrochloride into a colored azo dye. Derivatized HONO then flows into a long path absorption tube in which the absorption of light by the azo dye is measured
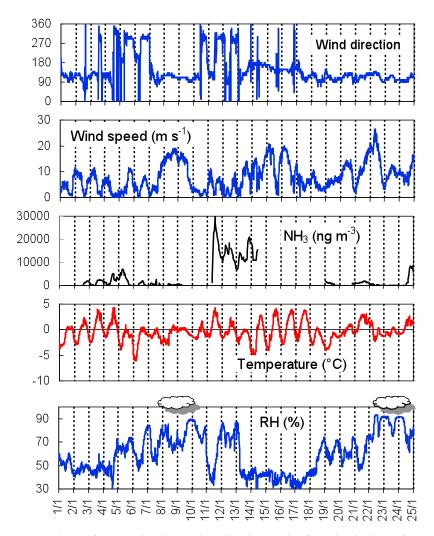
Figure 3. Concentrations of ammonia observed at the "iono" site from beginning of January 2011 to January 24, 2011 versus wind conditions, temperature and relative humidity. Periods of snowfalls are denoted with a symbol depicting cloudy conditions on top of radiation relative humidity (RH) plots.

by a spectrometer from 550 to 610 nm [*Heland et al.*, 2001]. More details can be found in *Kerbrat et al.* [2012].

[18] Important photochemical parameters, e.g., ozone and CO were also measured. Ozone measurements were made continuously with a UV absorption monitor (Thermo Electron Corporation model 49I, Franklin, Massachusetts). The data collected at 15 s intervals are reported here as 15 min averages. Atmospheric CO was measured every three minutes with a gas-chromatograph equipped with a mercuric oxide reduction detector (Trace Analytical, USA), with the same principle as the instrument described in detail in *Gros et al.* [1999]. The reproducibility of the measurement was tested by repeated analysis of calibration standards contained in high-pressure cylinders and was 2.0 ppbv for the range of mixing ratios observed at DDU. Samples were calibrated against a 58 ppbv high-pressure aluminum cylinder calibrated by the CSIRO on their own "CSIRO94" scale which is linked to the gravimetrically derived scale of NOAA [*Novelli et al.*, 1991]. The calibration gas was analyzed every 3 min (alternatively with the air sample) and each air sample was calibrated against the previous standard. Air was sampled from outside (5 m above ground level) with a 10 m Dekabon line (1/4″).

[19] Specific oxygenated volatile organic compounds, in particular acetone and acetaldehyde, were measured by a high-sensitivity PTR-MS (Proton Transfer Mass Spectrometry, IONICON, Austria). Working conditions applied during this campaign are detailed in *Legrand et al.* [2012].

[20] In the framework of the French environmental observation service CESOA (Etude du cycle atmosphérique du Soufre en relation avec le climat aux moyennes et hautes

Table 2. Mixing Ratios (Mean and Range) of Chemical Species Used in *Kukui et al.* [2012] to Discuss Sources and Sinks of OH and RO$_2$ Radicals[a]

	Mean (±1σ)	Range
H$_2$O$_2$	380 ± 140 pptv	145–1000 pptv
MHP	260 ± 80 pptv	75–550 pptv
HCHO	170 ± 50 pptv	70–500 pptv
CH$_3$CHO	304 ± 192 pptv	25–2138 pptv
CH$_3$COCH$_3$	209 ± 120 pptv	71–1249 pptv
CH$_3$COOH	100 ± 250 pptv	0–1950 pptv

[a]The records of other relevant species are shown in Figure 6 (ozone, DMS), Figure 2 (CO), and Figure 3 (NH$_3$) of this paper.
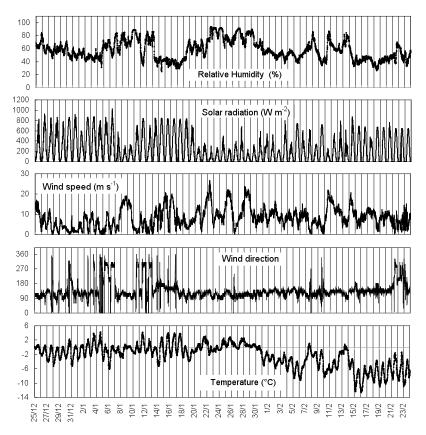
Figure 4. Weather conditions at Dumont d'Urville from end December 2010 to end February 2011. (top to bottom) Relative Humidity, Short Wave Solar Radiation, Wind Speed and Direction, and Temperature.

latitudes Sud, http://www.lgge.ujf-grenoble.fr/CESOA/rubrique.php3?id_rubrique=2) dedicated to the study of the sulfur cycle at middle and high southern latitudes, DMS was documented, at least once per day, by using a gas chromatograph equipped with a flame photometric detector (GCFP, see details in *Preunkert et al.* [2008]).

[21] Finally an URG-9000D Ambient Ion Monitor (AIM) was run to continuously investigate acidic gases, and NH_3, as well as aerosols, including particulate phase methanesulfonic acid (MSA). In brief, air is sucked through a liquid diffusion denuder where NH_3 and acidic gases are removed. Next, the air stream enters an aerosol super-saturation chamber where atmospheric aerosol grows and is subsequently trapped in a liquid water solution. Collected gas and aerosol are analyzed for anions and cations by using two ion chromatographs. More details can be found in *Legrand et al.* [2012]. For gaseous species like carboxylic acids a very good agreement was found by *Legrand et al.* [2012] when comparing AIM data with those gained by using other sampling techniques (glass denuder tubes, or mist chambers). Concerning aerosol, a very good agreement was found between AIM data and those obtained by sampling bulk aerosol on filters, as shown in section 3.2.2 for example for MSA.

3. Overview of Sampled Air Masses
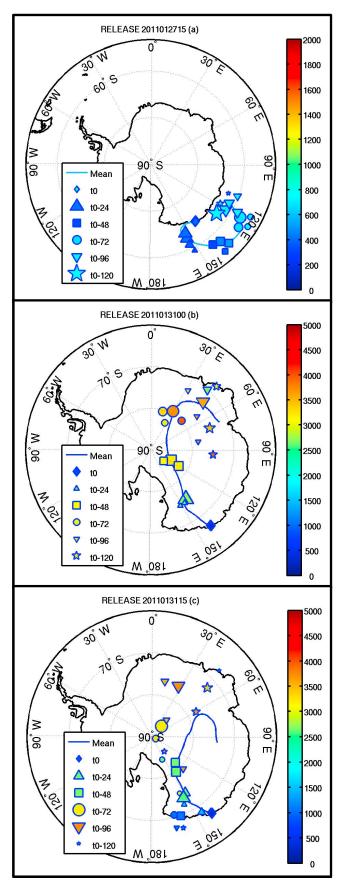
3.1. Local Meteorological Observations

[22] The beginning of summer 2010/2011 was characterized by bad weather conditions (snow storms) lasting November 20th followed by a period of sunny weather with low wind and largely positive temperatures during the day (up to 8°C December 12th). As discussed by *Legrand et al.* [2012] these conditions have favored optimal conditions for bacterial activity in ornithogenic soils and large emissions of ammonia, carboxylic acids, and acetaldehyde.

[23] Weather conditions encountered during the main sampling period (from the end December to mid January 2011) up to the HONO sampling time (from February 9th to February 23rd) are documented in Figure 4. Until January 7th weather was generally sunny except January 1st. January 7th a low-pressure system approached the Antarctic coast. January 8th and 9th were cloudy days with high wind speed (up to 20 m s^{-1}) and significant snowfalls (5 cm deposited early morning on January the 10th). For the rest of this period good weather conditions prevailed (except a little snow January 12th early morning).

[24] Whereas mild temperatures maintained during the second half of January, after 5 sunny days weather was most of time cloudy and several snowfalls occurred between January 22nd and January 29th. A regular temperature drop and cloudy conditions characterized the first week of February. Then temperatures warmed up and a snowfall occurred February 8th. At the beginning of the HONO sampling time (from February 9th to February 23rd) a little snow fell (10th and 13th) and then sunny weather conditions returned but accompanied by a decrease in temperatures.

[25] It therefore appears that sunny and dry conditions without snow fall maintained most of the time both during the OH (first half of January) and the HONO (second half

Figure 5. (a) Back trajectories from the FLEXPART model for a marine origin on 27/01/2011 15 UT, (b) a well-defined continental one on 31/01/2011 00 UT, and (c) a continental one with larger uncertainty on 31/01/2011 15 UT. The position and altitude (color scale in m) of the cloud of 1000 particles at time t0 are represented using a clustering technique. Five clusters are shown every 24 h with the same symbol the size of which is proportional to the number of particles associated to the cluster.
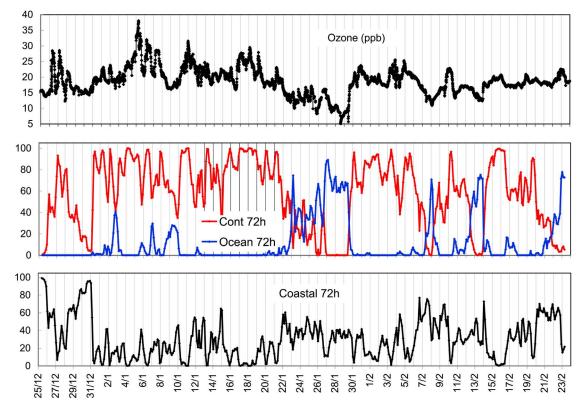
of February) measurement periods. The two periods experienced at least one time bad weather conditions with significant snowfalls. Similar meteorological conditions make the use of the range of HONO concentrations relevant for the OH data analysis.

3.2. Types of Sampled Air Masses

3.2.1. Methodology

[26] As previously discussed by *Legrand et al.* [2009], relatively high summer ozone levels (up to 35–40 ppbv) at DDU linked to the influence of continental air masses represent a unique feature compared to other coastal Antarctic regions where typical summer values remain close to 15 ppbv at that season. Local wind direction at DDU is not a sufficient tool to decide whether air masses are from marine or continental origin: moderate continental airflow is in general deviated to the east following the local glacier orography and arrives at DDU in a sector between 100 and 130°E and the corresponding air mass will be wrongly attributed to oceanic sources [see, e.g., *Pépy*, 2011]. Therefore, we have used the FLEXPART Lagrangian model (version 6) to assess the respective influence of the inland flow and of the marine flow. The FLEXPART model has been developed at NILU [*Stohl et al.*, 2005]. The model is run in a backward mode for 5 days and using a domain filling method where the atmosphere at the receptor location is represented by particles of equal mass. The transport and diffusion of particles is calculated using the 6-hourly ECMWF analyses (T213L91 i.e., 0.5 degree horizontal resolution and 20 model vertical levels below 3000 m) interleaved with operational forecasts every 3 h. We did not include any dry or wet deposition of the tracer, but the parameterization of sub grid dynamical processes and convection were included. Wind data from ECMWF analysis are known to underestimate katabatic winds near the surface in Antarctica [*Cullather et al.*, 1997]; thus the Lagrangian model based on these wind fields will not reproduce very well the true transport pathway, and the exact origin of the air parcel, but it still can distinguish faithfully marine and continental air masses. We have released 1000 particles every 3 h at altitudes between 0 and 500 m and in a 50 × 50 km area around DDU from December 24th 2010 (00 UT) to February 22nd 2011 (21 UT). We modified the FLEXPART model to introduce the calculation of the fraction of particles originating from two areas: inland continental Antarctica excluding the Ross sea (latitude lower than 70°S, longitude between 50°W et 170°E, altitude lower than 4000 m) and the marine boundary layer not including the coastal region (latitude between 50°S and 67°S, altitude lower than 1000 m). This fraction is calculated at each time step for a given release. The air mass origin analysis is mainly based on the fractions

Figure 6. (top) Ozone mixing ratios observed at "labo 3" from end December 2010 to late February 2011 versus (middle and bottom) the history of air masses as derived from Flexpart simulations (see section 3.2). Figure 6 (middle) refers to the fraction of particles originating from oceanic area (ocean 72 h) and continental area (cont 72 h) 72 h before observations. Figure 6 (bottom) refers to the sum fraction of particles originating neither from oceanic nor continental area (coastal 72 h).

calculated at 72 h before the DDU observations. We selected fractions at 72 h because longer time scales correspond to larger uncertainties on the air mass origins and time scales less than 48 h cannot discriminate between clear marine and continental distant sources. There are only small differences between the 48 h and 72 h fraction values. Air masses where both fractions are low correspond to a coastal influence from the Ross Sea or from the eastern coast of Antarctica. Three examples of the temporal evolution of the spatial distribution of 1000 particles released at DDU are shown in Figure 5 using a clustering technique (at a given time step up to 5 clusters with a fraction of particles more than 10% are represented). Compared to other trajectory tools, the FLEXPART dispersion model makes possible the identification of ambiguous cases when clusters with equal size are widespread at time step less than 3–4 days. For these cases, the exact origin of the air parcels may be not reconstructed precisely by FLEXPART, but the corresponding air masses are then not included in the high continental fraction cases which is used in this paper. The good comparison between calculated air mass origins and ozone levels observed in this paper provides also an additional validation of the air mass attribution technique based on this calculated continental fraction (see Figure 6). Low ozone levels indeed correspond to marine influenced periods and higher ones to continental air mass influence [*Legrand et al.*, 2009].

3.2.2. Results

[27] With the aim to investigate the origin of air masses sampled during the field measurement campaign, we report in Figure 6 the results from the trajectory/dispersion FLEXPART model and the ozone record at DDU. Over the main sampling time period with the OH instrument that ended mid-January, air masses mainly originated from inland Antarctica as shown by the large values of the continental air masses (cont 72 h in Figure 6). During the first week (end of December 2011) however there were a few days when the air mass were coming from coastal regions as depicted by the high value of the fraction of particles neither oceanic nor continental. During those days (December 25th, 29th, and 30th) ozone mixing ratios remained rather low (15 ppbv). Afterwards ozone level exhibited sudden increases (up to more than 10 ppbv) on December 26th, 27th, and 28th during the morning hours. They correspond to an increasing continental character of the air mass with respect to late afternoon when ozone was close to 15 ppbv. As seen in Figure 7, high MSA concentrations (200 ng m^{-3}) were present in air masses originating from coastal regions compared to very low ones (<50 ng m^{-3}) measured in air masses coming from inland Antarctica.

[28] January started with continental conditions until January 5th with only two sporadic marine inputs (January 1st afternoon and late January 2nd). Over these 5 days, the ozone mixing ratio gradually increased. During the next
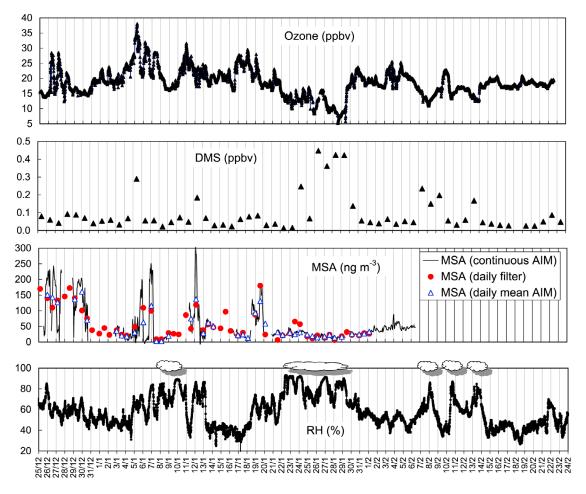
Figure 7. Ozone mixing ratio, DMS mixing ratios, MSA concentrations and relative humidity observed from late December 2010 to early February 2011. Periods of snowfalls are denoted with a symbol depicting cloudy conditions on top of relative humidity (RH) plots. In the MSA series, the black line corresponds to hourly mean sampling done with the AIM sampler, the red dots to bulk aerosol filter sampling (24 h), and the blue triangles to daily averaged AIM data.

three days (January 5th, 6th, and 7th) the high ozone levels observed each early morning suddenly dropped in the afternoon (by 16, 11, and 7 ppbv, respectively) in relation with an enhanced marine contribution. Similarly to end December two of these marine inputs are well detected in the MSA record (Figure 7). The January 7–9th snowstorm (see section 3.1) is related to the most important marine event of the main sampling period according to the FLEXPART simulations. While there was again low ozone level observed at DDU, the January 7th to 9th event was not accompanied by enhancement of MSA aerosol in contrast to previous marine events (see Figure 7). It is also the case during the last week of January when several significant snowfalls took place. This absence of MSA in marine air masses is likely due to scavenging of aerosol by snowfall.

[29] Continental conditions persisted until January 22th followed by 5 days in a row with marine events not seen before. The absolute minimum level of ozone (around 10 ppbv, Figure 6) was observed during this period. Note also that highest mixing ratios of DMS (400–500 pptv, Figure 7) were also observed end of January. Continental conditions returned from January 30th until February 6th.

[30] During the HONO sampling period, which took place from February 9th to February 23rd the origin of air masses, was very variable with an important marine contribution February 13th rapidly followed by a quasi-pure continental air mass arriving at night January 14th. Again this change from marine to continental was accompanied by a jump of the ozone level (Figure 6). Note however that this time the ozone increase remained quite moderate with respect to those having occurred in December or January. It is consistent with the weakening of photochemical ozone production inland East Antarctica in February pointed out by *Legrand et al.* [2009].

[31] In summary, during both the OH and HONO periods, continental air masses were very often sampled, particularly during the OH period. During the two periods air masses with significant coastal and marine contributions were also sampled.

4. First HO_x and HONO Measurements at DDU

4.1. OH Observations

[32] With average values of 2.1×10^6 and 3.3×10^8 molecule cm^{-3} for OH and RO_2, respectively, the OH and RO_2 concentrations observed at DDU by *Kukui et al.* [2012]

are the highest ever seen at the Antarctic coast. On the basis of steady state calculations, the observed high concentrations of RO_2 at DDU are in good agreement with the observed levels of O_3 and HCHO since their photolysis represent the major primary radical source. However, the OH level observed at DDU cannot be simply explained by the relatively high level of ozone observed at this site in relation with an efficient transport of air masses coming from inland Antarctica. For instance, the OH daily average at DDU would be about 7×10^5 molecule cm^{-3} when accounting only for the primary OH sources and the observed OH level requires a significant RO_2 to OH conversion mechanism. As neither NO nor halogen oxides were measured at DDU, the mechanism of this recycling could not be explicitly identified. However, the analysis of the origin of sampled air masses shows that the OH recycling is more efficient in continental air mass. This is consistent with the role of NO_x chemistry in the recycling as NO_x levels are expected to be far higher over the Antarctic plateau than over the surrounding oceans [*Wang et al.*, 2007]. The steady state concentration analysis implies a RO_2 to OH conversion mechanism equivalent to the presence of NO in the range from 10 to 50 pptv to explain observed OH and RO_2 concentrations.

4.2. HONO Observations

[33] Unlike the other compounds, HONO was measured at both the coastal site of DDU and the inland site of Concordia. As detailed in *Kerbrat et al.* [2012], whereas data reveal temporal changes that are consistent with changes of vertical mixing within the boundary layer at DC and with the origin of air masses (continental versus marine) at DDU, they do not confirm however the expected low HONO levels. Thus, the use of a LOPAP instrument unexpectedly did not permit to solve the issue related to the role of HONO on the oxidative capacity of the Antarctic atmosphere.

4.3. Perspectives

[34] During the second OPALE campaign carried out at Concordia in December 2011–January 2012, investigations have included measurements of OH and HO_2+RO_2 together with species relevant to discuss their sources and sinks (NO, NO_2, HONO, O_3, H_2O_2, HCHO), surface meteorological parameters and physic of the boundary layer, and photolysis rates. These data will complement the results of this first special issue and will allow a better understanding of the role of snowpack emissions on the oxidative properties of the atmosphere overlying the East Antarctic plateau. This will be discussed in a further set of papers.

References

Berresheim, H., and F. L. Eisele (1998), Sulfur Chemistry in the Antarctic Troposphere Experiment: An overview of project SCATE, *J. Geophys. Res.*, *103*, 1619–1627, doi:10.1029/97JD00103.

Bloomfield, P., and W. L. Steiger (1983), *Last Absolute Deviations: Theories, Applications, and Algorithms*, Birkhauser, Boston, Mass.

Bloss, W. J., J. D. Lee, D. E. Heard, R. A. Salmon, S. J. B. Bauguitte, H. K. Roscoe, and A. E. Jones (2007), Observations of OH and HO_2 radicals in coastal Antarctica, *Atmos. Chem. Phys.*, *7*, 4171–4185, doi:10.5194/acp-7-4171-2007.

Charlson, R. J., J. E. Lovelock, M. O. Andreae, and S. G. Warren (1987), Ocean phytoplankton, atmospheric sulphur, cloud albedo and climate, *Nature*, *326*, 655–661, doi:10.1038/326655a0.

Chen, G., et al. (2001), An investigation of South Pole HO_x chemistry: Comparison of model results with ISCAT observations, *Geophys. Res. Lett.*, *28*(19), 3633–3636, doi:10.1029/2001GL013158.

Chen, G., et al. (2004), A reassessment of HO_x South Pole chemistry based on observations recorded during ISCAT, *Atmos. Environ.*, *38*, 5451–5461, doi:10.1016/j.atmosenv.2003.07.018.

Cullather, R. I., D. H. Bromwich, and R. W. Grumbine (1997), Validation of operational numerical analyses in Antarctic latitudes, *J. Geophys. Res.*, *102*(D12), 13,761–13,784, doi:10.1029/96JD03328.

Davis, D. D., et al. (2001), Unexpected high levels of NO observed at South Pole, *Geophys. Res. Lett.*, *28*(19), 3625–3628, doi:10.1029/2000GL012584.

Davis, D. D., et al. (2004), An overview of ISCAT 2000, *Atmos. Environ.*, *38*, 5363–5373, doi:10.1016/j.atmosenv.2004.05.037.

Davis, D. D., et al. (2008), A reassessment of Antarctic plateau reactive nitrogen based on ANTCI 2003 airborne and ground based measurements, *Atmos. Environ.*, *42*, 2831–2848, doi:10.1016/j.atmosenv.2007.07.039.

Gros, V., B. Bonsang, and R. Sarda-Esteve (1999), Atmospheric carbon monoxide 'in situ' monitoring by automatic gas chromatography, *Chemosphere Global Change Sci.*, *1*(1–3), 153–161, doi:10.1016/S1465-9972(99)00010-0.

Heland, J., J. Kleffmann, R. Kurtenbach, and P. Wiesen (2001), A new instrument to measure gaseous nitrous acid (HONO) in the atmosphere, *Environ. Sci. Technol.*, *35*(15), 3207–3212, doi:10.1021/es000303t.

Jefferson, A., D. J. Taner, F. L. Eisele, D. D. Davis, G. Chen, J. Crawford, J. W. Huey, A. L. Torres, and H. Berresheim (1998), OH photochemistry and methane sulfonic acid formation in the coastal Antarctic boundary layer, *J. Geophys. Res.*, *103*, 1647–1656, doi:10.1029/97JD02376.

Jourdain, B., and M. Legrand (2001), Seasonal variations of dimethyl sulfide, dimethyl sulfoxide, sulfur dioxide, methanesulfonate, and non-sea-salt sulfate aerosols at Dumont d'Urville (December 1998–July 1999), *J. Geophys. Res.*, *106*, 14,391–14,408, doi:10.1029/2000JD900841.

Jourdain, B., and M. Legrand (2002), Year-round records of bulk and size-segregated aerosol composition and HCl and HNO_3 levels in the Dumont d'Urville (coastal Antarctica) atmosphere: Implications for sea-salt aerosol in the winter and summer, *J. Geophys. Res.*, *107*(D22), 4645, doi:10.1029/2002JD002471.

Kerbrat, M., M. Legrand, S. Preunkert, H. Gallée, and J. Kleffmann (2012), Nitrous acid at Concordia on the East Antarctic Plateau and its transport to the coastal site of Dumont d'Urville, *J. Geophys. Res.*, *117*, D08303, doi:10.1029/2011JD017149.

Kukui, A., G. Ancellet, and G. Le Bras (2008), Chemical ionisation mass spectrometer for measurements of OH and peroxy radical concentrations in moderately polluted atmospheres, *J. Atmos. Chem.*, *61*(2), 133–154, doi:10.1007/s10874-009-9130-9.

Kukui, A., M. Legrand, G. Ancellet, V. Gros, S. Bekki, R. Sarda-Estève, R. Loisil, and S. Preunkert (2012), Measurements of OH and RO_2 radicals at the coastal Antarctic site of Dumont d'Urville (East Antarctica) in summer, *J. Geophys. Res.*, *117*, D12310, doi:10.1029/2012JD017614.

Lazrus, A. L., G. L. Kok, S. N. Gitlin, and J. A. Lind (1985), Automated fluorometric method for hydrogen peroxide in atmospheric precipitation, *Anal. Chem.*, *57*, 917–922, doi:10.1021/ac00281a031.

Legrand, M. (1997), Ice-core records of atmospheric sulphur, *Philos. Trans. R. Soc., Ser. B*, *352*, 241–250, doi:10.1098/rstb.1997.0019.

Legrand, M., and P. Mayewski (1997), Glaciochemistry of polar ice cores: A review, *Rev. Geophys.*, *35*, 219–243, doi:10.1029/96RG03527.

Legrand, M., F. Ducroz, D. Wagenbach, R. Mulvaney, and J. Hall (1998), Ammonium in coastal Antarctic aerosol and snow: Role of polar ocean and penguin emissions, *J. Geophys. Res.*, *103*, 11,043–11,056, doi:10.1029/97JD01976.

Legrand, M., S. Preunkert, B. Jourdain, H. Gallée, F. Goutail, R. Weller, and J. Savarino (2009), Year round record of surface ozone at coastal (Dumont d'Urville) and inland (Concordia) sites in East Antarctica, *J. Geophys. Res.*, *114*, D20306, doi:10.1029/2008JD011667.

Legrand, M., V. Gros, S. Preunkert, R. Sarda-Estève, A.-M. Thierry, G. Pépy, and B. Jourdain (2012), A reassessment of the budget of formic and acetic acids in the boundary layer at Dumont d'Urville (coastal

Antarctica): The role of penguin emissions on the budget of several oxygenated volatile organic compounds, *J. Geophys. Res.*, *117*, D06308, doi:10.1029/2011JD017102.

Mauldin, R. L., III, et al. (2001a), Measurements of OH, H_2SO_4, and MSA at the South Pole during ISCAT, *Atmos. Environ.*, *28*, 3629–3632.

Mauldin, R. L., III, et al. (2001b), Measurements of OH aboard the NASA P-3 during PEM-Tropics B, *J. Geophys. Res.*, *106*, 32,657–32,666, doi:10.1029/2000JD900832.

Novelli, P. C., J. W. Elkins, and L. P. Steele (1991), The development and evaluation of a gravimetric reference scale for measurements of atmospheric carbon monoxide, *J. Geophys. Res.*, *96*, 13,109–13,121, doi:10.1029/91JD01108.

Pépy, G. (2011), Etude du formaldéhyde en zone côtière Antarctique, PhD thesis, 251 pp., Univ. Joseph Fourier de Grenoble, Grenoble, France.

Preunkert, S., M. Legrand, B. Jourdain, C. Moulin, S. Belviso, N. Kasamatsu, M. Fukuchi, and T. Hirawake (2007), Interannual variability of dimethyl-sulfide in air and seawater and its atmospheric oxidation by-products (methanesulfonate and sulfate) at Dumont d'Urville, coastal Antarctica (1999–2003), *J. Geophys. Res.*, *112*, D06306, doi:10.1029/2006JD007585.

Preunkert, S., B. Jourdain, M. Legrand, R. Udisti, S. Becagli, and O. Cerri (2008), Seasonality of sulfur species (sulfate, methanesulfonate and dimethyl sulfur) in Antarctica: Inland versus coastal regions, *J. Geophys. Res.*, *113*, D15302, doi:10.1029/2008JD009937.

Riedel, K., R. Weller, and O. Schrems (1999), Variability of formaldehyde in the Antarctic troposphere, *Phys. Chem. Chem. Phys.*, *1*, 5523–5527, doi:10.1039/a905368i.

Riedel, K., R. Weller, O. Schrems, and G. König-Langlo (2000), Variability of tropospheric hydroperoxides at a coastal surface site in Antarctica, *Atmos. Environ.*, *34*, 5225–5234, doi:10.1016/S1352-2310(00)00322-8.

Salmon, R. A., S. J.-B. Bauguitte, W. Bloss, M. A. Hutterli, A. E. Jones, K. Read, and E. W. Wolff (2008), Measurement and interpretation of gas phase formaldehyde concentrations obtained during the CHABLIS campaign in coastal Antarctica, *Atmos. Chem. Phys.*, *8*, 4085–4093, doi:10.5194/acp-8-4085-2008.

Stohl, A., C. Forster, A. Frank, P. Seibert, and G. Wotawa (2005), Technical note: The Lagrangian particle dispersion model FLEXPART version 6.2, *Atmos. Chem. Phys.*, *5*, 2461–2474, doi:10.5194/acp-5-2461-2005.

Tuncel, G., N. K. Aras, and W. H. Zoller (1989), Temporal variations and sources of elements in the South Pole atmosphere: 1. Nonenriched and moderately enriched elements, *J. Geophys. Res.*, *94*(D10), 13,025–13,038, doi:10.1029/JD094iD10p13025.

Wagenbach, D. (1996), Coastal Antarctica: Atmospheric chemical composition and atmospheric transport, in *Chemical Exchange Between the Atmosphere and Polar Snow*, *NATO ASI Ser.*, vol. 43, edited by E. W. Wolff and R. C. Bales, pp. 173–199, Springer, Berlin.

Wang, Y., Y. Choi, T. Zeng, D. Davis, M. Buhr, L. G. Huey, and W. Neff (2007), Assessing the photochemical impact of snow NO_x emissions over Antarctica during ANTCI 2003, *Atmos. Environ.*, *41*, 3944–3958, doi:10.1016/j.atmosenv.2007.01.056.

Weller, R., and D. Wagenbach (2007), Year-round chemical aerosol records in continental Antarctica obtained by automatic samplings, *Tellus, Ser. B*, *59*, 755–765, doi:10.111/j.1600-0889.2007.00293.x.

Weller, R., D. Wagenbach, M. Legrand, C. Elsässer, X. Tian-Kunze, and G. König-Langlo (2011), Continuous 25-years aerosol records at coastal Antarctica: Part 1. Inter-annual variability of ionic compounds and links to climate indices (2011), *Tellus, Ser. B*, *63*, 901–919, doi:10.1111/j.1600-0889.2011.00542.x.

Wolff, E. W., et al. (2006), Southern ocean sea-ice extent, productivity and iron flux over the past eight glacial cycles, *Nature*, *440*, 491–496, doi:10.1038/nature04614.